Supporting Information

Wolschner et al. 10.1073/pnas.0902688106

SI Materials and Methods

Chemicals. Norleucine (Nle) was purchased from Sigma-Aldrich, and methoxinine (Mox) from CBL Patras. All other chemicals were from Sigma-Aldrich, Fluka, Biomol, and Merk, unless stated otherwise.

Expression of Full-Length Recombinant Human Cellular Prion Protein (rhPrP^C) and Media Composition. The expression of methionine Met-rhPrP^C, Nle-rhPrP^C, and Mox-rhPrP^C was performed by using the Met-auxotrophic *Escherichia coli* strain B834(DE3) (F^-*ompT hsdS*$_D$(r_D^- m_D^-) *gal dcm metE* λ(DE3) (Novagen Merck). Transformed host cells were grown in new minimal medium (NMM) (1), which contains 22 mM KH_2PO_4, 50 mM K_2HPO_4, 8.5 mM NaCl, 7.5 mM $(NH4)_2SO_4$, 1 mM $MgSO_4$, 20 mM glucose, 1 μg/mL Ca^{2+}, 1 μg/mL Fe^{2+}, 0.001 μg/mL trace elements (Cu^{2+}, Zn^{2+}, Mn^{2+}, MoO_4^{2-}), 10 μg/mL thiamin, 10 μg/mL biotin, and the appropriate antibiotics (100 μg/mL amicillin and 34 μg/mL chloramphenicol). The stock solutions of both Nle and Mox (100 mg/mL) were freshly made before usage, and routinely used for expression and incorporation at a concentration of 5.0 mM without special precautions.

Plasmids and PrP Sequence. *E. coli* B834(DE3) was cotransformed with 2 plasmids; first, the ampicillin resistant pET17b-hPrP(23–231)WT81 for human PrP23–231 M129 (2), which is under the control of the T7 promoter; and second, the chloramphenicol resistant rare codon plasmid, pRIL (Stratagene), which is a derivative of pACYC184 plasmid, and contains tRNA-genes for the rare Arg, Ile, and Leu codons (AGG, AGA, AUA, and CUA, respectively). The coding sequence of the recombinant full-length rhPrP^C(23–231) contains beside the codon for the initial methionine (Met; ref. 1) also serine (Ser; ref. 2) as second amino acid (3). This amino acid composition should facilitate N-terminal Met-excision (4), and subsequently increase protein stability against degradation, according to the N-End Rules (5). Therefore, the gene rhPrP^C(23–231) encodes for 211 aa, whereas in the purified proteins, N-terminal Met residue is expected to be excised.

Fermentation and Expression of Met-rhPrP^C, Nle-rhPrP^C, and Mox-rhPrP^C. All fermentation and expression experiments were performed in the above described synthetic medium (NMM). Transformed cells were grown in 5 mL LB-medium overnight with 100 μg/ml ampicillin and 34 μg/ml chloramphenicol; 100 μL of the overnight culture were used for the inoculation of 1 L NMM. Cells were grown to midlog phase (OD_{600} 0.6–0.8) in NMM containing limiting amounts (0.04 mM) of L-Met. Protein expression in Met starved cells was induced with 1 mM IPTG (Applichem) and 5.0 mM L-Met, D,L-Nle, or L-Mox was concomitantly added. Proteins expression was performed for 4 h or overnight at 30 °C with aeration achieved by vigorous shaking.

Protein Refolding and Purfication. Proteins were expressed in inclusion bodies. The isolation and refolding protocol was identical for all variants. Based on the published protocols (6), cells were harvested by centrifugation and resuspended in 20 mL of 50 mM Tris·HCl (pH 8.0) with 1 mM $MgCl_2$, and disrupted in a French pressure cell (15,000 psi; SLM-Aminco). The inclusion bodies were sedimented by centrifugation (25 min, 49,000 × *g*, 4 °C), and washed twice with 50 mM Tris·HCl (pH 8.0), 23% (wt/vol) sucrose, 0.5% (vol/vol) Triton X-100, 1 mM EDTA, 1 mM benzamidine. The pellet was dissolved in 8 M urea, 10 mM Mops (pH 7.0), 50 mM DTT and 1 mM EDTA, and was centrifuged (30 min, 130,000 × *g*, 22 °C). The supernatant was applied to linked Fractogel EMD-DEAE and Fractogel EMD-SO_3 ion exchange columns (Merck KGaA), 25 and 15 mL, respectively, which were equilibrated in 8 M urea and 10 mM Mops (pH 7.0). Proteins were eluted from the Fractogel EMD-SO_3 column with 8 M urea, 10 mM Mops (pH 7.0) and 500 mM NaCl. All fractions containing solubilized rhPrP^{C}s were pooled and diluted in 8 M urea, 500 mM NaCl, and 100 mM Tris·HCl (pH 8.5) to a protein concentration of 0.05 mg/mL. Subsequently, the $CuSO_4$ was added to a final concentration of 2 μM, and the solution was stirred for 4 h at room temperature. As a result, the formation of the single disulfide bond takes place. The oxidation reaction was quenched by addition of 1 mM EDTA. Excessive EDTA was bound with the addition of 1 mM NiAc, and pH was adjusted to about 6.8 with 1 M HCl. The oxidized PrPs were applied to 5 mL Chelating Sepharose Fast Flow (GE Healthcare), precharged with NiAc according to the manufacturer's recommendations and preequilibrated with 8 M urea, 500 mM NaCl, and 10 mM Mops pH 7.0. The bound proteins were eluted with 8 M urea, 500 mM NaCl, 10 mM Mops pH 7.0, and 250 mM imidazole. Protein containing fractions were pooled, and refolding was done in 50-fold volume in 10 mM Mes pH 6.0 at 4 °C overnight. Refolded proteins were concentrated and stored at 4 °C.

Protein Purity and Concentration Determination. The purity of the recombinant protein samples was demonstrated by SDS PAGE, HPLC analysis and electrospray ionization mass spectrometry (ESI-MS) analysis. Concentrations of Met-rhPrP^C samples were determined using a PerkinElmer Lambda 17 UV/VIS spectrophotometer assuming an extinction coefficient of 57932.5 $M^{-1}cm^{-1}$, as calculated from the amino acid composition using SwissProtParam software tools. Protein concentrations were calculated as described elsewhere (7).

ESI-MS. The extent of replacement of the native Met-residues by Nle or Mox was confirmed by high-resolution mass analysis using liquid chromatography (LC) coupled with the ESI-time of flight (TOF) MS MicroTOF-LC from Bruker Daltonics. Samples were separated by Symmetry C4 column (Waters) with a flow rate of 250 μL/min and 15 min linear gradient from 20–80% acetonitrile/0.05% trifluoroacetic acid.

CD Spectroscopy and Melting Curves. The far-UV CD spectra of full-length rhPrP^{C}s were recorded on a dichrograph JASCO J-715 (JASCO International). All spectra are averages of 4 scans, and are reported as mean residue molar ellipticity ($[\theta]_R$) in degrees × cm^2 × $dmol^{-1}$. Quartz cells (110-QS Hellma) of 0.1 cm optical path length and protein concentrations of 8.73 μM were used. Ellipticity changes were recorded between 200 and 260 nm at 37 °C in 10 mM Mes pH 6.0. Melting curves were determined by monitoring the changes in dichroic intensity at 222 nm in function of temperature increase. Thermal denaturation experiments were performed in the range from 4 to 95 °C, with a heating rate of 30 °C h^{-1}. Temperature was controlled by a JASCO Peltier type FDCD attachment (model PFD-350S/350L). The fractions of unfolded protein were calculated from the corresponding ellipticity data, as well as the midpoint of denaturation (melting temperature or T_m value) (6).

Fluorescent Labeling of rhPrP^C. Protein labeling was performed with the amino-reactive fluorescent dyes Alexa Fluor-488- and Alexa Fluor-647-O-succinimidylester (Molecular Probes), respectively. The fluorescent dyes (2 mg/mL in DMSO) were added to a solution of 8.73 μM rhPrP^C at a molar ratio of 3:1. After incubation for 2 h at room temperature, unbound fluorophores were separated by 2 filtration steps in Microspin columns filled with Sephadex G25 (Amersham Pharmacia Biotech), equilibrated with 20 mM sodium phosphate buffer (pH 7.2) containing 0.2% SDS (Sigma). Removal of unbound dye molecules and labeling efficiency were confirmed by FCS and SIFT measurements on an Insight Reader (Evotec-Technologies).

FCS/SIFT Measurements and Analysis. FCS and SIFT measurements were carried out (Insight Reader; Evotec-Technologies) with dual-color excitation at 488 and 633 nm, using a 40 $\times$ 1.2 NA microscope objective (Olympus) and a pinhole diameter of 70 μm at FIDA setting. Excitation power was 200 μW at 488 nm, and 300 μW at 633 nm. Measurement time was 5 $\times$ 10 s. For scanned measurements, scanning parameters were set to 100 μm scan path length, 50 Hz beamscanner frequency, and 2,000 μm positioning table movement. This is equivalent to $\approx$10 mm/s scanning speed. The temperature for all measurements was 20–25 °C. The fluorescence data were analyzed by correlation analysis using the FCSPPE valuation software version 2.0 (Evotec OAI) as described (8). Two-color cross-correlation amplitudes G(0) were determined using the same software. Evaluation of SIFT data in 2D intensity distribution histograms was performed as described previously (9). To quantify aggregate formation, cross-correlation analysis was used, because dual-color cross-correlation analysis allows more sensitive detection and quantification than single-color autocorrelation analysis. Also, cross-correlation analysis can be combined with scanning, which further improves sensitivity of aggregate detection (10).

Aggregation Assay. Stock solutions of rhPrP^C labeled as described above were prepared in 20 mM sodium phosphate buffer (pH 7.2) containing 0.2% SDS. The concentration of rhPrP^C-Alexa 488 was $\approx$20 molecules per focal volume, whereas rhPrP^C-Alexa 647 was adjusted to 30 molecules per focal volume. SIFT measurements confirmed that the stock solution was free of rhPrP^C aggregates. Experiments were performed by diluting the stock solutions, in buffer containing 0 or 0.2% SDS, to obtain final SDS concentrations of 0.0125 and 0.2% SDS, respectively. Experiments were done in 96-well-plates with a cover slide bottom (Evotec-Technologies). To reduce evaporation, the 96-well-plates were sealed with adhesive film. Aggregation was monitored for about 12 h using 4 parallel and identical samples for each experimental group.

Aggregation Assay in Different Periodate Concentrations ($NaIO_4$). The experimental setup was performed as described before. The only difference was that different volumes of $NaIO_4$ stock solution (100 μM and 50 mM) were pipeted during the first dilution step in order to give final concentrations of 2 μM, 200 μM, and 10 mM $NaIO_4$ in the examined samples.

1. Budisa N, et al. (1995) High-level biosynthetic substitution of methionine in proteins by its analogs 2-aminohexanoic acid, selenomethionine, telluromethionine and ethionine in Escherichia-coli. *Eur J Biochem* 230:788–796.
2. Giese A, Levin J, Bertsch U, Kretzschmar H (2004) Effect of metal ions on de novo aggregation of full-length prion protein. *Biochem Biophys Res Commun* 320:1240–1246 320:1240–1246.
3. Hornemann S, Glockshuber R (1996) Autonomous and reversible folding of a soluble amino-terminally truncated segment of the mouse prion protein. *J Mol Biol* 261:614–619.
4. Merkel L, Cheburkin Y, Wiltschi B, Budisa B (2007) In vivo chemoenzymatic control of n-terminal processing in recombinant human epidermal growth factor. *ChemBioChem* 8:2227–2232.
5. Varshavsky A (1992) The n-end rule. *Cell* 69:725–735.
6. Liemann S, Glockshuber R (1999) Influence of amino acid substitutions related to inherited human prion diseases on the thermodynamic stability of the cellular prion protein. *Biochemistry* 38:3258–3267.
7. Tahiri-Alaoui A, Gill AC, Disterer P, James W (2004) Methionine 129 variant of human prion protein oligomerizes more rapidly than the valine 129 variant - implications for disease susceptibility to creutzfeldt-jakob disease. *J Biol Chem* 279:31390–31397.
8. Schwille P, MeyerAlmes FJ, Rigler R (1997) Dual-color fluorescence cross-correlation spectroscopy for multicomponent diffusional analysis in solution. *Biophys J* 72:1878–1886.
9. Bieschke J, et al. (2000) Ultrasensitive detection of pathological prion protein aggregates by dual-color scanning for intensely fluorescent targets. *Proc Natl Acad Sci USA* 97:5468–5473.
10. Giese A, Bieschke J, Eigen M, Kretzschmar HA (2000) Putting prions into focus: Application of single molecule detection to the diagnosis of prion diseases. *Arch Virol* (Suppl 1):161–171.

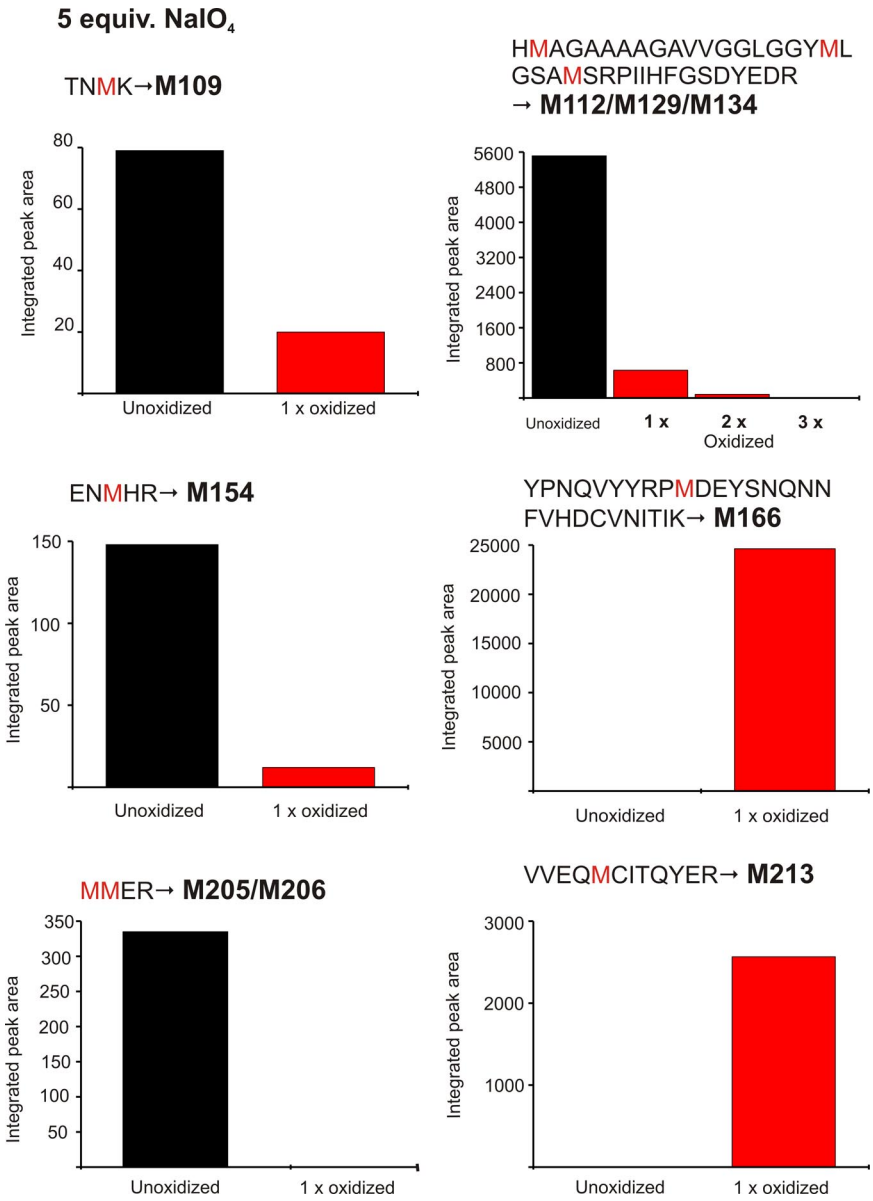

Fig. S1. Schematic representation of the oxidation level of the generated Met-rhPrP^{C} peptides, using peak area integration from mass spectra as analysis tool. The protein was oxidized using 5 eq of $NaIO_4$, and peptides were generated by tryptic digestion.

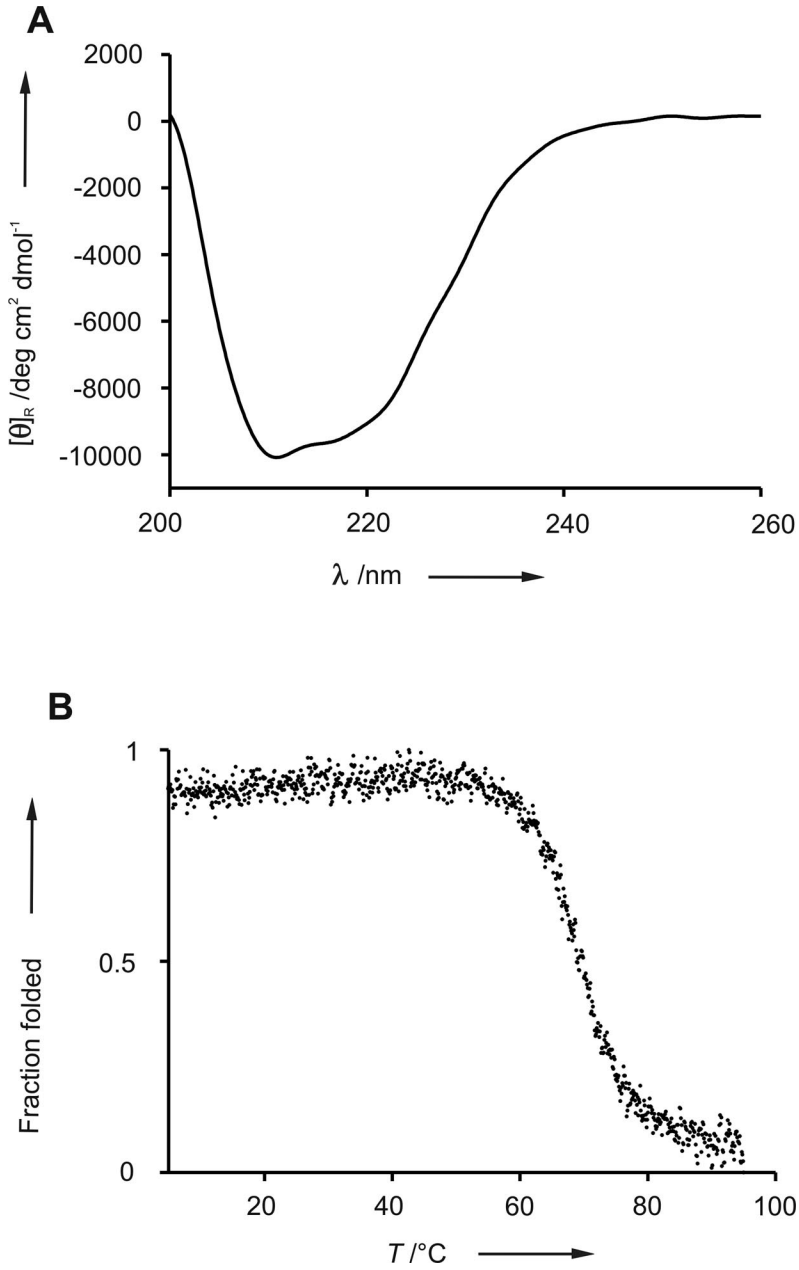

Fig. S2. Secondary structure and thermally induced unfoding profile of Met-rhPrP^C treated with 5 eq of $NaIO_4$. (*A*) Secondary structure of Met-rhPrP^C (c = 0.2 mg/mL) after overnight treatment with 5 eq of $NaIO_4$, measured by far-UV CD spectroscopy. (*B*) Thermally induced unfolding profile of $NaIO_4$ treated Met-rhPrP^C (T_m = 68.8 °C). The fraction of unfolded protein was calculated from CD data monitored at 222 nm, as described in the experimental section.

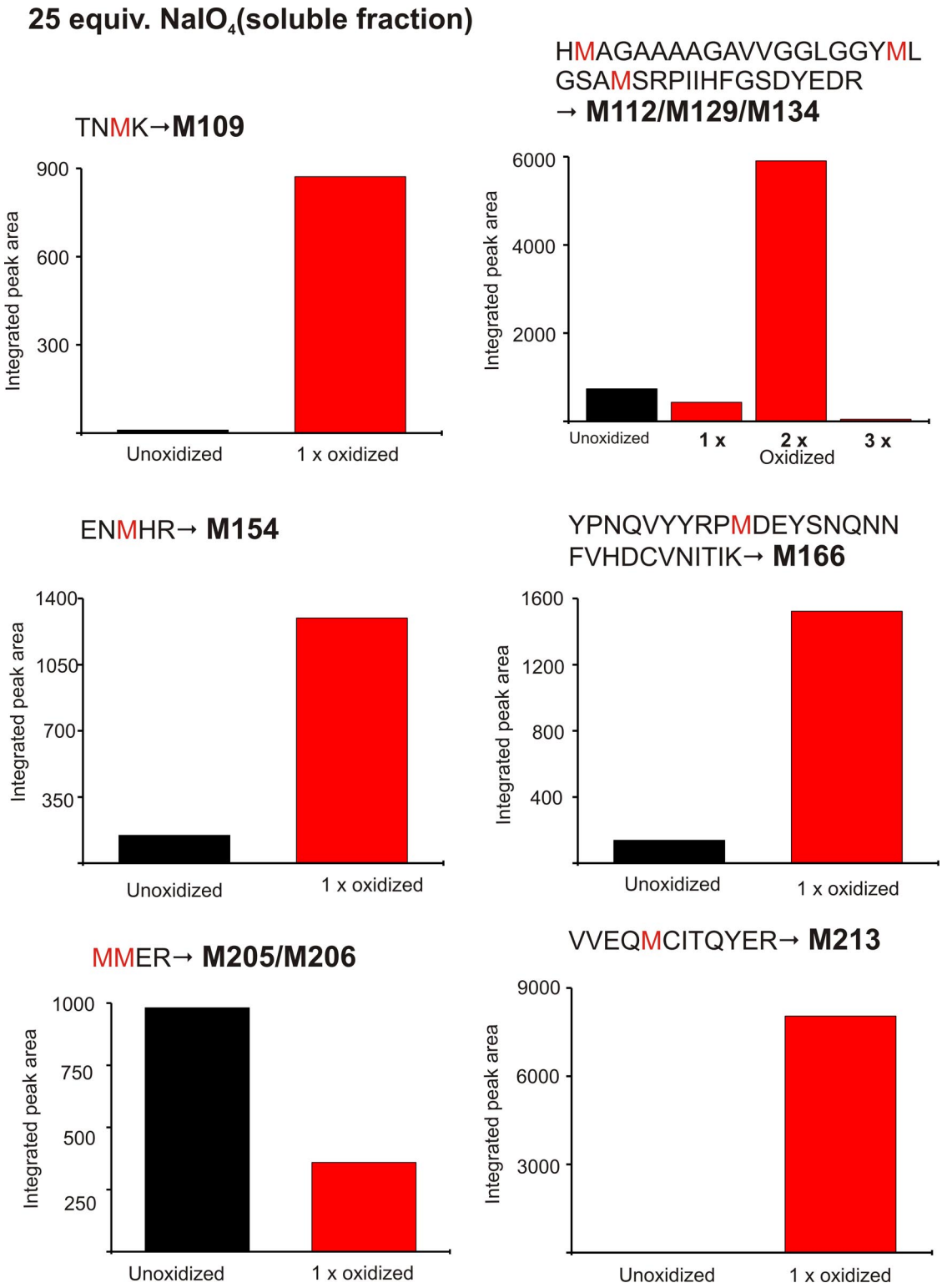

Fig. S3. Schematic representation of the oxidation level of the tryptic Met-rhPrP^{C} peptides, using peak area integration from mass spectra as analysis tool. The protein was oxidized using 25 eq of $NaIO_4$ (soluble fraction), and peptides were generated by tryptic digestion.

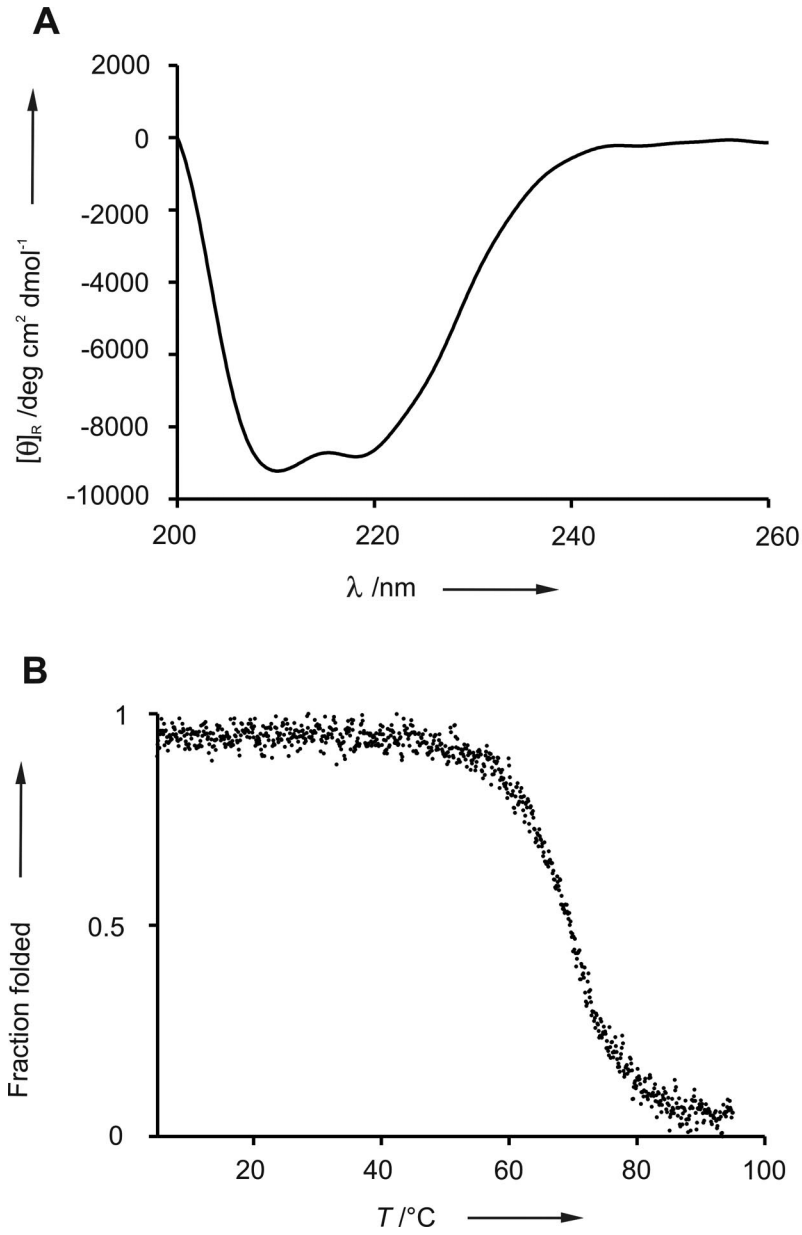

Fig. S4. Secondary structure and thermally induced unfoding profile of Met-rhPrP^C treated with 25 eq of $NaIO_4$. (*A*) Secondary structure of Met-rhPrP^C (c = 0.2 mg/mL) after overnight treatment with 25 eq of $NaIO_4$ (soluble fraction), measured by far-UV CD spectroscopy. (*B*) Thermally induced unfolding profile of $NaIO_4$ treated Met-rhPrP^C (T_m = 69.5 °C). The fraction of unfolded protein was calculated from CD data monitored at 222 nm, as described in the experimental section.

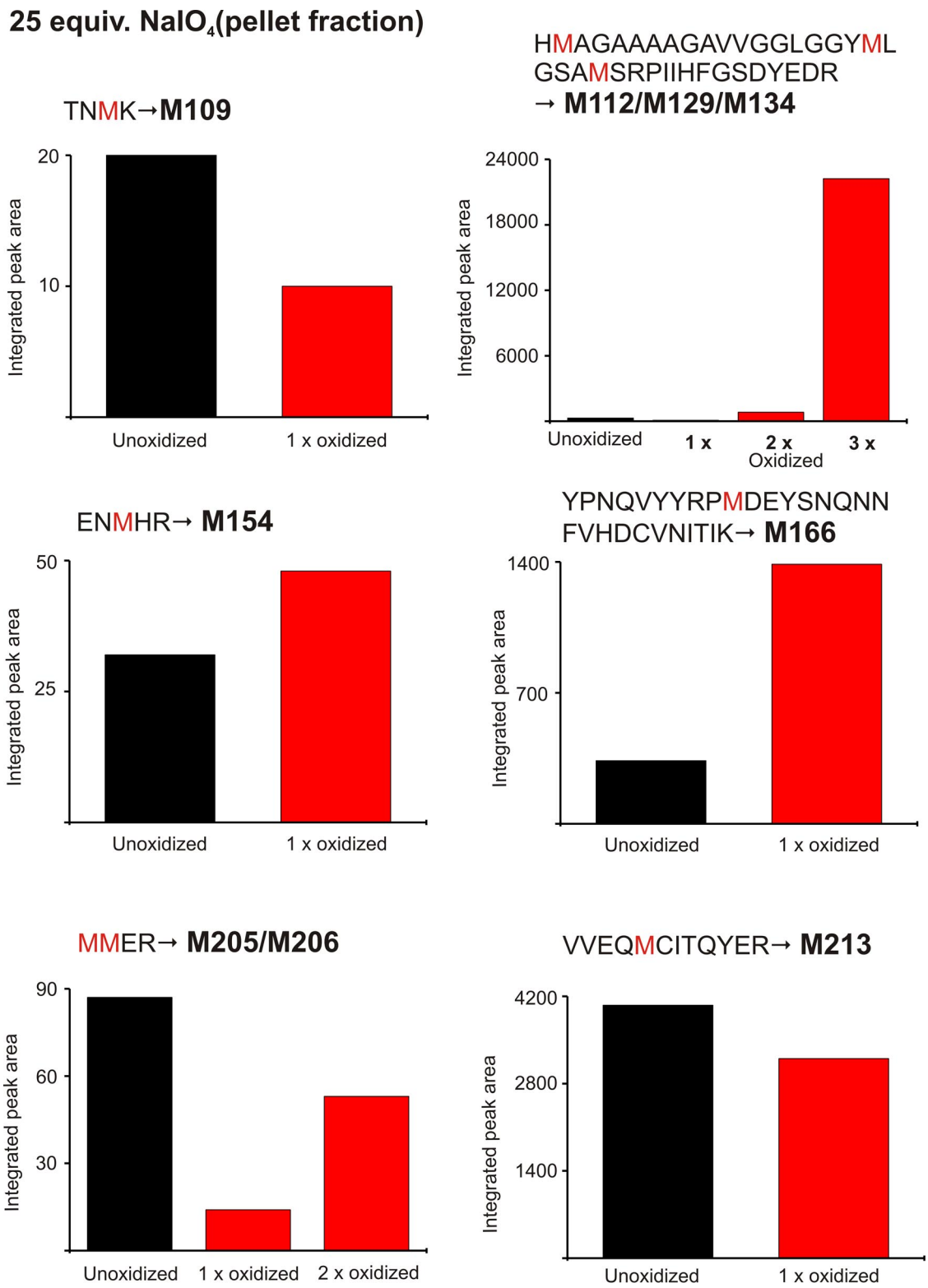

Fig. S5. Graphical representation of the oxidation level of the tryptic Met-rhPrP^{C} peptides, using peak area integration from mass spectra as analysis tool. The protein was oxidized using 25 eq of $NaIO_4$ (pellet fraction), and peptides were generated by tryptic digestion.

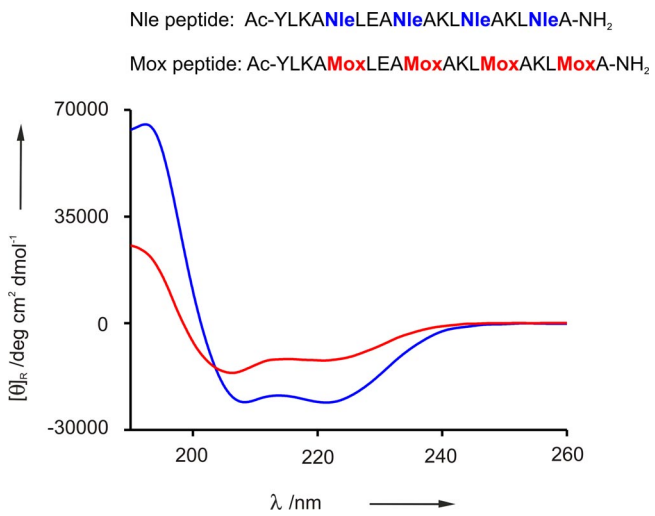

Fig. S6. Secondary structure of 2 variants, Nle (blue) and Mox (red), of the 18 aa model peptide (c = 100 μM; 20 °C), measured by far-UV CD spectroscopy.

Table S1. Calculated composition of the different secondary structures of the 2 peptide analogues, Nle (blue) and Mox (red), of the Dado–Gellmann model peptide, as computed with the CONTIN software (Reference SMP56)/CDPro Analysis

190–260 nm	Nle, %	Mox, %
Helix	84.3	38.1
Antiparallel	0.1	3.8
Parallel	1.6	6.8
Beta-Turn	8.7	19.2
Rndm. Coil	5.3	32.1